Photodissociation dynamics of hydroxybenzoic acids

Yi Lin Yang,[1,a)] Yuri Dyakov,[1] Y. T. Lee,[1,a)] Chi-Kung Ni,[1,b)] Yi-Lun Sun,[2] and Wei-Ping Hu[2,c)]
[1]*Institute of Atomic and Molecular Sciences, Academia Sinica, Taipei 10617, Taiwan*
[2]*Department of Chemistry and Biochemistry, National Chung Cheng University, Chia-Yi 621, Taiwan*

(Received 23 August 2010; accepted 20 November 2010; published online 21 January 2011)

Aromatic amino acids have large UV absorption cross-sections and low fluorescence quantum yields. Ultrafast internal conversion, which transforms electronic excitation energy to vibrational energy, was assumed to account for the photostability of amino acids. Recent theoretical and experimental investigations suggested that low fluorescence quantum yields of phenol (chromophore of tyrosine) are due to the dissociation from a repulsive excited state. Radicals generated from dissociation may undergo undesired reactions. It contradicts the observed photostability of amino acids. In this work, we explored the photodissociation dynamics of the tyrosine chromophores, 2-, 3- and 4-hydroxybenzoic acid in a molecular beam at 193 nm using multimass ion imaging techniques. We demonstrated that dissociation from the excited state is effectively quenched for the conformers of hydroxybenzoic acids with intramolecular hydrogen bonding. *Ab initio* calculations show that the excited state and the ground state potential energy surfaces change significantly for the conformers with intramolecular hydrogen bonding. It shows the importance of intramolecular hydrogen bond in the excited state dynamics and provides an alternative molecular mechanism for the photostability of aromatic amino acids upon irradiation of ultraviolet photons. © *2011 American Institute of Physics*. [doi:10.1063/1.3526059]

I. INTRODUCTION

Although aromatic amino acids such as tyrosine have large UV absorption cross-sections, the respective fluorescence quantum yields are small; indicating the presence of fast nonradiative processes which efficiently quench the fluorescence.[1–4] The nonradiative process is assumed to be ultrafast internal conversion.[2–5] Following internal conversion (electronic-to-vibrational energy transfer) the highly vibrationally excited molecules quickly dissipate their energy to surrounding molecules through intermolecular energy transfer before chemical reactions initiate. This so-called photostability prevents the undesired photochemical reactions for these molecules upon the irradiation with ultraviolet photons. However, recent theoretical calculations[6–10] suggested that the low fluorescence quantum yields for phenol and indole (chromophores for tyrosine and tryptophan) is due to dissociation from a repulsive excited electronic state, rather than fast internal conversion to the ground electronic state. Dissociation from a repulsive excited state has been verified in recent molecular beam experiments.[11–14] Since this type of dissociation is swift, quenching is incomplete even in the condensed phase. As a result, chemical reactions following the generation of radicals from the dissociation become an obstacle to the photostability of amino acids. An alternative explanation for the photostability of amino acids seems to be necessary.

Unlike phenol, aromatic amino acids such as tyrosine found in peptides and proteins all have additional long and floppy functional groups. For example, tyrosine has a CH_2CHNH_2COOH group in addition to the phenol moiety. These molecules have many conformers, which typically interconvert via hindered rotations about single bonds. Some of them can form intramolecular or intermolecular hydrogen bonding. Low barriers for interconversion, relative to the energy for photoexcitation or chemical transformation, result in fast equilibrium for the various conformers. Consequently, similar photochemical properties are usually expected for different conformers. Recently, it was found that the UV absorption spectra of the aromatic amino acids, as well as of small peptides containing aromatic amino acids, can exhibit a pronounced dependence on the ground-state conformation.[15–23] On the other hand, only few examples of conformationally controlled photodissociation have been observed,[24–26] and they are not amino acid related molecules. Little discussion has been directed at the conformationally controlled photodissociation of amino acids.

In this work, photodissociation of tyrosine chromophores, 2-hydroxybenzoic acid (2-HBA), 3-hydroxybenzoic acid (3-HBA), and 4-hydroxybenzoic acid (4-HBA) are investigated in a molecular beam at 193 nm using multimass ion imaging techniques. (The structures of three molecules can be found in the figure below.) Hydrogen atom elimination from a repulsive excited state is the major channel for the majority of the conformers. This dissociation mechanism is similar to the hydrogen atom elimination for phenol. However, we found that hydrogen atom elimination channel of 2-HBA conformers with intramolecular hydrogen bonding is nearly quenched. *Ab initio* calculations show that

[a)]Also at Department of Chemistry, National Taiwan University, Taipei 10617, Taiwan.
[b)]Author to whom correspondence should be addressed. Electronic mail: ckni@po.iams.sinica.edu.tw. Also at Department of Chemistry, National Tsing Hua University, Hsinchu, Taiwan.
[c)]Author to whom correspondence should be addressed. Electronic mail: chewph@ccu.edu.tw.

these conformers have significantly different potential energy surfaces. The implication of intramolecular hydrogen bonding effects on the photostability of amino acid chromophores upon the irradiation of UV photons is discussed.

II. EXPERIMENTS

The experimental techniques have been described in details elsewhere.[27–29] Basically molecules in a molecular beam are photodissociated using a pulsed UV laser beam set at 193 nm. The resulting photofragments are ionized with a pulsed VUV laser beam at 118 nm. Photofragment masses are identified along with their translational energy distributions using multimass ion imaging techniques.

Because the vapor pressure of the hydroxybenzoic acids is very low at room temperature, it is necessary to heat them in order to increase their concentration in the molecular beam. However, these compounds decompose easily on metal surface at high temperature. A specially designed high temperature pulsed nozzle is used to generate high concentration of each compound in the molecular beam. A stainless steel oven maintained at ~100 °C is attached to the exit port of a commercial pulsed nozzle (General valve series 9). The front surface of the nozzle is covered with a 5 mm thickness polyimide and the inner surface of the oven is coated with graphite. The plunger of the pulsed nozzle made by polyimide passes through the 5 mm thick polyimide and extends to the exit port of the oven to control the opening of the oven. Each compound is mixed with graphite powder before loading into the oven. Ultra pure Ne at a pressure of 250 Torr flowed from the nozzle to the oven. The sample/rare gas mixture is expanded through the exit port of the oven forming the molecular beam. The VUV photoionization and time-of-flight (TOF) mass spectrum are used to check the content of the molecular beam before the photodissociation experiment is initiated.

III. THEORETICAL CALCULATION

Ground state geometries for various conformers and the corresponding interconversion transition states were calculated with the B3LYP/6–31G method.[30,31] Energies of these structures then were refined by the G3(MP2,CCSD) scheme.[32,33] All ground-state electronic structure calculations were performed using the Gaussian 03 package.[34]

The excited-state energy calculation was done using the complete active space (CAS) theory with the 6-31+G(d,p) basis set. The active space consists of 12π electrons and 12 orbitals (6π, 4π*, and 2σ*). A state averaged approach with equal weighting was applied to calculate the two lowest states of A′ and A″ symmetry simultaneously. This calculation was carried out using the MOLPRO 2009 program.[35] For some nonplanar structures of 2HBA, the time-dependent (TD)[36] B3LYP theory with 6-311+G(d,p) basis set was applied to calculate the ground- and excited-state energies for a more consistent comparison to the energies of the planar structures and due to the consideration of computational resources. The TD-B3LYP calculation was performed using the Gaussian 03 package.

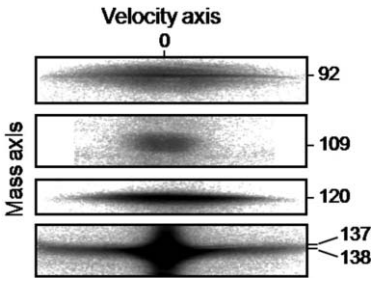

FIG. 1. Photofragment ion images of 2-HBA. Pump and probe laser pulse delay time are 38, 19, 38, and 100 μs for m/z = 92, 109, 120, and 137, respectively.

IV. RESULTS

A. 2-hydroxybenzoic acid (2-HBA)

The VUV photoionization/time-of-flight mass spectra of 2-HBA reveal that there is little contamination in the molecular beam. Only a small amount of photofragment ion $m/z = 120$ was observed. It is from the dissociative ionization of the parent ion by excess VUV photon energy $C_6H_4OHCOOH + h\nu$ (118 nm) $\rightarrow C_6H_4OCO^+$ (m/z = 120) + H_2O. This process is not rapid and it occurs during the ion acceleration within the ion optics, resulting in the broadening of the feature of the TOF mass spectra. Only trace amounts of impurities (e.g., $m/z = 92$) were observed, likely due to the thermal decomposition of parent molecules in the oven. See Fig. S1(a) of supplementary material for the corresponding mass spectra.[37]

Photofragment ions $m/z = 64$, 92, 109, 120, and 137 were observed from the dissociation of 2-HBA at 193 nm using 118 nm ionization photons. Ions $m/z = 64$, 92, and 120 have large intensities, and 109 and 137 have small intensities. The relative ion intensities of these fragments can be measured from the TOF mass spectra, as illustrated in Fig. S1(b) of supplementary material.[37] Photolysis laser fluence in the region of 1–9.5 mJ/cm^2 was used in ion imaging measurement to determine the photolysis photon number dependence of each fragment. It showed that only fragments $m/z = 64$ result from two-photon absorption with all the other fragments originating from one-photon absorption. In view of this, the discussion of our findings concentrates exclusively on dissociation channels resulting from one-photon absorption.

Images for various fragments are shown in Fig. 1. The image of m/z = 137 was weakly observed, due to a small signal and interference from parent ion m/z = 138. It is a line shape image, representing the dissociation channel: $C_6H_4OHCOOH + h\nu$ (193 nm) $\rightarrow C_6H_4OCOOH$ (m = 137) + H. The photofragment translational energy distribution is illustrated in Fig. 2(a). Ion image of m/z = 120 is also a line shape image and represents the H_2O elimination channel: $C_6H_4OHCOOH + h\nu$ (193 nm) $\rightarrow C_6H_4OCO$ (m = 120) + H_2O. The translational energy distribution is shown in Fig. 2(b). Fragment $m/z = 109$ has a disk-like image. The width of the disk changes with delay time. It represents the dissociative ionization of heavy fragments (from H

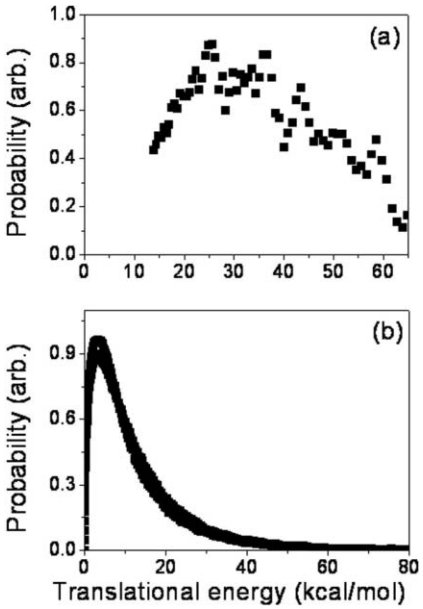

FIG. 2. Photofragment translational energy distribution of 2-HBA for reaction (a) $C_6H_4OHCOOH \rightarrow C_6H_4OCOOH + H$. (b) $C_6H_4OHCOOH \rightarrow C_6H_4OCO + H_2O$.

elimination channel) by VUV photoionization: $C_6H_4OCOOH + hv$ (118 nm) $\rightarrow C_6H_5O_2^+$ ($m/z = 109$) + CO. The image for fragment $m/z = 92$ contains both line-shape and disk-like components. The line-shape image represents three body dissociation, $C_6H_4OHCOOH + hv$ (193 nm) $\rightarrow C_6H_4O$ ($m = 92$) + H_2O + CO. The disk-like image represents the dissociative ionization of heavy fragments from H_2O elimination channel: C_6H_4OCO ($m = 120$) + hv (118 nm) $\rightarrow C_6H_4O^+$ ($m/z = 92$) + CO.

B. 3-hydroxybenzoic acid (3-HBA)

The VUV photoionization/time-of-flight mass spectra for 3-HBA shows that only minor impurities ($m/z = 92$) due to thermal decomposition of parent molecules in the oven exist in the molecular beam. See Fig. S2 of supplementary material for the corresponding mass spectra.[37]

Only photofragment ion $m/z = 137$ was observed from the dissociation of 3-HBA at 193 nm using 118 nm ionization photons. The ion image as shown in Fig. 3 represents the dissociation channel: $C_6H_4OHCOOH + hv$ (193 nm) $\rightarrow C_6H_4OCOOH$ ($m = 137$) + H. The corresponding photofragment translational energy distribution is illustrated in Fig. 4. It shows a large portion of fast component and a small portion of slow component. The slow component is strongly interfered by the parent ion with the actual amount being smaller than that shown in Fig. 4. The peak for the fast

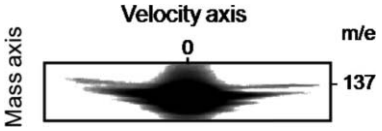

FIG. 3. Photofragment ion images of 3-HBA. Pump and probe laser pulse delay time is 92 μs.

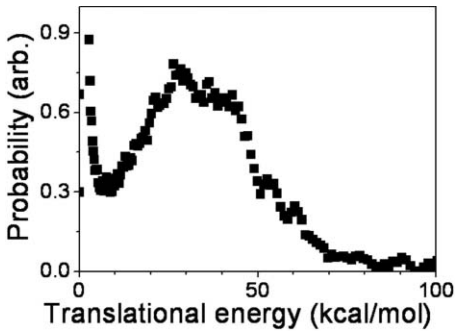

FIG. 4. Photofragment translational energy distribution of 3-HBA for reaction $C_6H_4OHCOOH \rightarrow C_6H_4OCOOH + H$.

component is located at 35 kcal/mol. The maximum energy release is close to that for the maximum available energy. The large translational energy release is consistent with the premise for dissociation from a repulsive excited state.

C. 4-hydroxybenzoic acid (4-HBA)

The VUV photoionization/time-of-flight mass spectra of 4-HBA show that only a trace amount of impurities ($m/z = 94$) observed; likely due to the thermal decomposition of parent molecules in the oven: $C_6H_4OHCOOH \rightarrow C_6H_5OH + CO_2$. See Fig. S3(a) of supplementary material for the corresponding mass spectra.[37]

Photofragment ions $m/z = 65$, 81, 109, 121, and 137 were observed from the dissociation of 4-HBA at 193 nm using 118 nm ionization photons. Ion $m/z = 137$ have the largest intensity. The other fragment ion intensities are two to three times smaller than $m/z = 137$ intensity. The relative ion intensities of these fragments are illustrated in Fig. S3(b) of supplementary material.[37] Photolysis laser fluence in the region of 1–8.3 mJ/cm^2 was used in ion imaging measurement to determine the photon number dependence of the fragments. These results confirmed that these fragments were entirely from one-photon absorption.

The images of various fragments are shown in Fig. 5. Image of $m/z = 137$ has the largest intensity and pertains to the dissociation channel: $C_6H_4OHCOOH + hv$ (193 nm)

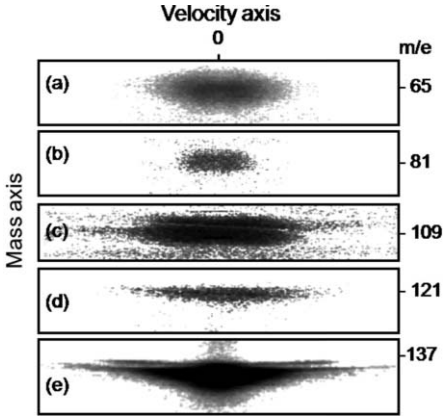

FIG. 5. Photofragment ion images of 4-HBA. Pump and probe laser pulse delay time are 35 μs for (a) and (b), and 83 μs for (c)–(e).

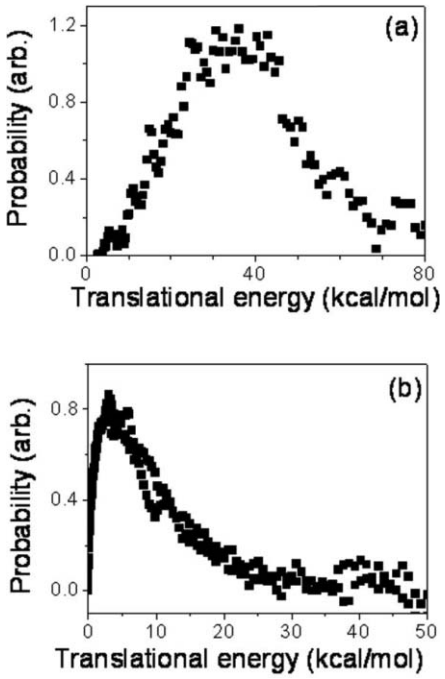

FIG. 6. Photofragment translational energy distribution of 4-HBA for reaction (a) $C_6H_4OHCOOH \rightarrow C_6H_4OCOOH + H$ (b) $C_6H_4OHCOOH \rightarrow C_6H_4OHCO + OH$.

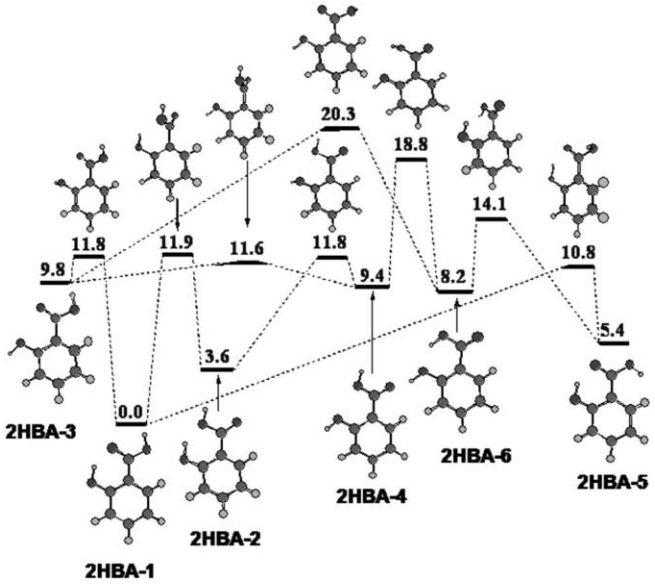

FIG. 7. The structures, energies of various conformers and barriers of 2-HBA.

$\rightarrow C_6H_4OCOOH$ ($m = 137$) + H. The photofragment translational energy distribution is illustrated in Fig. 6(a). Ion image of $m/z = 121$ has a line-shape image. It represents the OH elimination channel: $C_6H_4OHCOOH + h\nu$ (193 nm) $\rightarrow C_6H_4OHCO$ ($m = 121$) + OH. The photofragment translational energy distribution for this channel is shown in Fig. 6(b). The fragments $m/z = 109$, 81, and 65 have disk-like images with their widths changing with delay time between pump and probe laser pulses. They result from the dissociative ionization of heavy fragments of H elimination channel by VUV photoionization: $C_6H_4OCOOH + h\nu$ (118 nm) $\rightarrow C_6H_5O_2^+$ ($m/z = 109$) +CO, $C_6H_4OCOOH + h\nu$ (118 nm) $\rightarrow C_5H_5O^+$ ($m/z = 81$) + 2CO, and $C_6H_4OCOOH + h\nu$ (118 nm) $\rightarrow C_5H_5^+$ ($m/z = 65$) + CO + CO_2, respectively.

D. Structures and energies of conformers

Different orientation of hydroxyl and carboxyl groups in hydroxybenzoic acids results in many conformers. 2-HBA has eight conformers. The calculated structures, relative energies, and barrier heights between these conformers are shown in Fig. 7. The proximity of the hydroxyl and carboxyl groups in 2-HBA leads itself to intramolecular hydrogen bonding. These bonds can be formed as such: O–H—O=COH or O–H—O(H)C=O, as for 2-HBA-1. 2HBA-2 and 2-HBA-5. Two conformers of 2-HBA are not stable, and they are not shown in Fig. 7. One has a geometry in which the hydroxyl group and the OH portion of the carboxyl group point toward each other. The other has a structure similar to 2-HBA-3, but the OH portion of the carboxyl group points toward to the aromatic ring. This structure is not stable from the calculation by G3 method, but it is stable in the B3LYP/6–31G* level calculation with a very small barrier (<1 kcal/mol) and it converts to 2-HBA-6 easily. Energies are higher by 5–10 kcal/mol for 2-HBA conformers without intramolecular hydrogen bonding (e.g., 2-HBA-3, 2-HBA-4, and 2HBA-6) than the 2-HBA conformers where intramolecular molecular hydrogen bonding is present.

The hydroxyl and carboxyl groups in 3-HBA and 4-HBA are too distant from one another for intramolecular hydrogen bonding to be a factor. As a result, even the most stable conformers of 3-HBA and 4-HBA are 4∼6 kcal/mol higher in energy than that the conformer 2-HBA-1. 3-HBA also has eight conformers and 4-HBA has only four conformers due to the symmetry. See Figs. S4 and S5 of supplementary material for the calculated structures, relative energies, and barrier heights between these conformers.[37] The 3-HBA conformers can be divided into two groups, depending on whether the OH portion of the carboxyl group points toward or away from the aromatic ring. Those conformers for which OH points away from the aromatic ring (e.g., 3-HBA-1, 3-HBA-2, 3-HBA-3, and 3-HBA-4) have energies ∼5 kcal/mol lower than conformers for which OH is directed toward the aromatic ring (e.g., 3-HBA-5, 3-HBA-6, 3-HBA-7, and 3-HBA-8). The direction of the hydroxyl group in 3-HBA appears to be unimportant with respect to the conformation energy. A similar trend in conformation energy is also observed for 4-HBA.

Barrier heights between comformers are in the range of 3–12 kcal/mol. The energy difference between conformers with hydrogen bonding and without hydrogen bonding is sufficiently large such that most of 2-HBA remains as 2-HBA-1 at room temperature. On the other hand, various conformers of 3-HBA (i.e., 3-HBA-1, 3-HBA-2, 3-HBA-3, and 3-HBA-4) and 4-HBA (i.e., 4-HBA-1 and 4-HBA-2) coexist at room temperature. Since the vibrational temperature in the molecular beam is much lower than the room temperature (estimated to be less than 100 K), almost all 2HBA molecules have the structure like 2-HBA-1 in the molecular beam, whereas

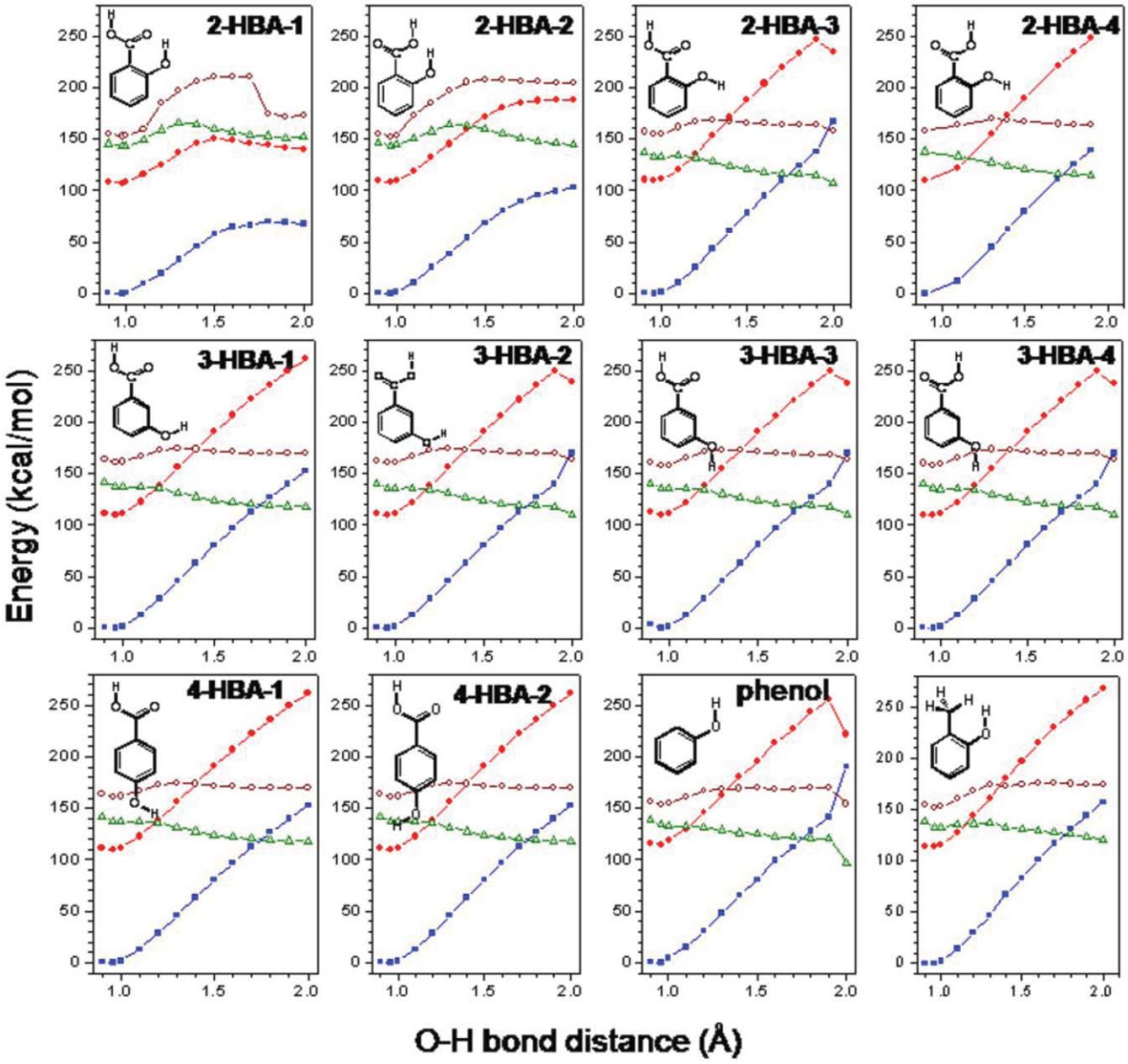

FIG. 8. The energies (kcal/mol) of the ground state and singlet excited states along the O-H bond distance (Å) in hydroxyl group. The solid squares, solid circles, open triangles and open circles represent 1A′, 2A′, 1A″, and 2A″, respectively.

various conformers of 3-HBA and 4-HBA coexist in the molecular beam.

E. Excited state potential energy along the (hydroxyl) O–H bond

We calculated the PES for the ground state and the singlet excited states along the O–H bond distance of hydroxyl group for various conformers of HBA, as shown in Fig. 8. Calculations also include PES for phenol and 2-methylphenol for comparison.

For phenol, the figure shows that the lowest singlet excited state 2A′ is bound and its second excited state 1A″ is repulsive. The 1A″ state crosses 2A′ at short O–H bond distance (∼1.1 Å) and then crosses the ground state at large O–H bond distance (∼1.8 Å). This result is the same as the previous investigation.[8] Concerning 3-HBA, 4-HBA, 2-methylphenol, and the 2-HBA conformers without intramolecular hydrogen bonding (e.g., 2-HBA-3 and 2-HBA-4), calculations showed that the lowest singlet excited state 2A′ is bound and the second excited state 1A″ is repulsive. The 1A″ state crosses 2A′ at short O–H bond distance and then crosses the ground state at large O–H bond distance. This result is similar to that of phenol. Hydrogen atom elimination initiates via the population transfer from the bright state 2A′ to the dark state 1A″, and then to the 1A′ ground state. The sum of these two population transfer processes results in the H-atom elimination on a repulsive potential energy surface, producing ground-state products with large translational energies. Energy at the crossing point between 1A″ and 2A′ is about 135 kcal/mol relative to the ground-state energy minimum. It is about 120 kcal/mol above the ground-state energy minimum at the crossing point between 1A″ state and the ground state.

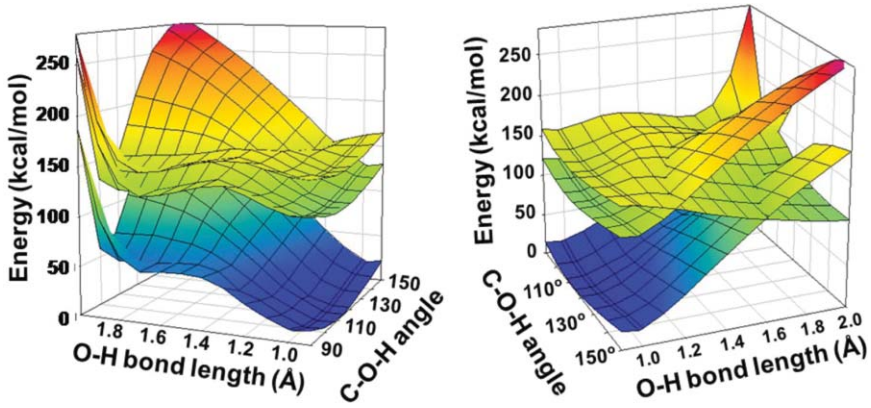

FIG. 9. The potential energy surfaces of 2-HBA-1 along O–H bond distance and C–O–H angle in hydroxyl group.

By contrast, the properties of the PES are very different for the 2-HBA comformers with intramolecular hydrogen bonding (e.g., 2-HBA-1 and 2-HBA-2). For these confromers, the 1A″ state becomes a bound state at short O–H bond distances. The energy barrier for the change from bound to repulsive is as large as ∼160 kcal/mol (relative to the ground-state energy minimum), thereby exceeding the 193 nm photon energy (148 kcal/mol). In addition, at large O–H bond distances, the ground-state potential energies of these hydrogen-bonded conformers do not increase as rapidly as the non-hydrogen-bonded conformers. At large O–H distances, the formation of zwitterionic like species such as Ph=O(–)...(+)HO=COH or Ph=O(–)...(+)H2OC(O)H might be more favorable for the hydrogen-bonded conformers. This reduces the ground-state energy significantly at large O–H bond distance and avoids intersecting with the 1A" state. As a result, the H atom elimination from the repulsive excited state does not occur on the 1A" for the 2HBA conformers with intramolecular hydrogen bonding.

To explore the potential energy surfaces on geometries other than vicinity of the minimum energy structures on the ground-state, we calculated the potential energy curves as a function of both the O–H bond distance and C–O–H angle in the hydroxyl group. Two integrated 3-D plots viewed from different angles are shown in Fig. 9. The figure shows that the region of potential well on the 1A" state becomes smaller as the C–O–H angle increases. The 1A" becomes a repulsive state as the angle reaches 150°. This suggests that some of the 2-HBA-1 can dissociate into fragment through H-atom elimination channel if the C–O–H angle increases significantly on the excited state during the dissociation process. However, because the crossing point between the 1A″ and 2A′ states is as high as 150 kcal/mol, it is anticipated that H-atom elimination is not important for conformer 2-HBA-1 with intramolecular hydrogen bonding.

Calculation of PES was also performed as a function of both the hydroxyl O–H bond distance and the angle between O–H bond axis and the plane of the aromatic ring for 2-HBA-1. It shows that the 1A″ state remains as a bound state at short O–H bond distance and it does not cross with 2A′ state. As we rotate the hydroxyl group of 2-HBA out of the plane, the point group symmetry changes from C_S to C_1. The original 1A′ state (now the 3A state) has an avoided-crossing with the original 2A′ state (now the 2A state) due to symmetry constraints. The out-of-plane rotation also keeps the ground state surface well separated from the original dark state at most rotational angles. The 1A and 2A states do not cross until the hydroxyl group rotates 180 degrees and conformer 2-HBA-1 becomes conformer 2-HBA-3. See Fig. S6 of supplementary material for the details of the PES.[37] Although the conformation change is possible on the excited state, the weakly observed H atom elimination from 2-HBA-1 suggests that internal conversion to the ground state is much faster than the rotation of hydroxyl group on the excited state for 2HBA-1. The hydrogen atom elimination of 2HBA-1 from the excited state is almost completely quenched. Instead, dissociation on the ground electronic state becomes the major channel.

We also calculated similar potential curves for 2-methylphenol, as shown in Fig. 8. The conformers of 2-methylphenol that we calculated have structures in which the hydroxyl group points toward the methyl group. These structures are intended to imitate the geometry of 2-HBA-1. However, replacing the carboxyl group with a methyl group effectively eliminates the chance for intramolecular hydrogen bonding. The results reveal that the potential energy surfaces for the excited states are very similar to that for phenol and conformers of 2-HBA without intramolecular hydrogen bonding.

F. Excited state potential energy along the (carboxyl) O–H bond

Repulsive excited state PES along the O–H bond distance of carboxyl group was also investigated by *ab initio* calculation. However, the repulsive potential energy surface is located at much higher energy than the photon energy we used in this work, See Fig. S7 of supplementary material for detailed description.[37] The calculations confirm that H atom elimination only occurs from the hydroxyl group.

G. Potential energies for dissociation channels on the ground state

Calculations were performed for the potential energies of intermediates, transition states and products for the various dissociation channels of 2-HBA on the ground electronic

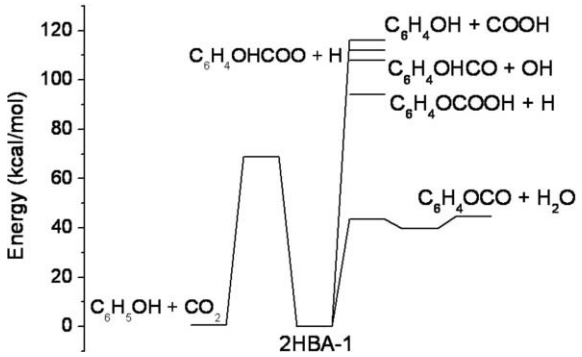

FIG. 10. Potential energies of intermediates, transition states, and products for various dissociation channels of 2-HBA on the electronic ground state.

state. They are shown in Fig. 10. The H_2O elimination from 2-HBA features a low barrier (~44 kcal/mol). This channel occurs through the movement of hydrogen atom from hydroxyl group toward the OH portion in carboxyl group, resulting in the product $C_6H_4(O)CO$ and H_2O. Another low-energy dissociation channel is the CO_2 elimination which has very small heat of reaction, $\Delta H = 0.6$ kcal/mol. However, the energy barrier is quite large (~68 kcal/mol). All the other dissociation channels (i.e., H, OH, and COOH eliminations) have large dissociation thresholds. The elimination of H_2O is the dominant channel for 2-HBA on the ground state due to the low dissociation barrier. On the other hand, the hydroxyl group is not sufficiently close to the carboxyl group in either 3-HBA or 4-HBA and therefore H_2O elimination requires extensive isomerization before the reaction can take place. Consequently, the energy barriers for H_2O elimination in both 3-HBA (87 kcal/mol) and 4-HBA (98 kcal/mol) are very large. The barrier heights and the dissociation thresholds for the remaining dissociation channels for 3-HBA and 4-HBA are not altogether different than those for 2-HBA. The CO_2 elimination, which maintains the lowest dissociation barrier for 3-HBA (74 kcal/mol) and 4-HBA (70 kcal/mol), becomes the major channel for 3-HBA and 4-HBA on the ground state. See Figs. S8 and S9 of supplementary material for the potential energy diagrams of 3-HBA and 4-HBA.[37]

V. DISCUSSION

A. Comparison to phenol and benzoic acid

Hydroxybenzoic acid contains both –OH and –COOH functional groups. A comparison of the dissociation properties for HBA to those for both phenol and benzoic acid reveals that a competition exists between these two functional groups in HBA. The photodissociation of phenol at 193 nm shows that the major dissociation channels include: H-atom, CO, and H_2O elimination; with greater than 70% of the H-atom elimination occurring on a repulsive excited state.[11] A small portion of phenol molecules become highly vibrationally excited in the ground state after internal conversion. Dissociation occurs on the ground state for channels with low barrier heights, including H- atom (89.1 kcal/mol), CO (84.0 kcal/mol), and H_2O (86.4 kcal/mol) elimination.

Three dissociation channels were observed from the photodissociation of benzoic acid at 193 nm: (1) $C_6H_5COOH \rightarrow C_6H_5 + COOH$, (2) $C_6H_5COOH \rightarrow C_6H_5CO + OH$, and (3) $C_6H_5COOH \rightarrow C_6H_6 + CO_2$.[38] Comparisons of experimental measurements with potential energies obtained from *ab initio* calculations and the branching ratios from the Rice–Ramsperger–Kassel–Marcus (RRKM) theory suggest that the first two dissociation channels occur on the electronic excited states and CO_2 elimination occurs on the ground state. The CO_2 elimination is the only dissociation pathway with a relatively low barrier height (71.7 kcal/mol) on the ground state. Dissociation barriers for the other elimination channels are significantly larger. Branching ratios for these channels are very small on the ground state. They include the following: CO elimination (87 kcal/mol), H_2O elimination (81 kcal/mol), H-atom elimination (107 kcal/mol), OH elimination (107 kcal/mol), and COOH elimination (108 kcal/mol).

A comparison of phenol, benzoic acid, and HBA shows that hydroxyl group plays a key role in HBA. For conformers of HBA that do not exhibit intramolecular hydrogen bonding, dissociation occurs only on the excited state and is dominated in large part by the hydroxyl group. For example, hydrogen atom elimination on the excited state is the major channel for both 3-HBA and 4-HBA. Only a small amount of OH elimination from carboxyl functional group in 4-HBA was observed. However, for 2-HBA conformers with intramolecular hydrogen bond, the H-atom elimination channel on the excited state is almost closed. Dissociation on the excited state, analogous to that for benzoic acid, does not occur, either. The COOH group remains as a spectator and does not play a role in the excited state dissociation dynamics. These conformers simply become highly vibrationally excited in the ground state. Dissociation occurs only through H_2O elimination, which has the lowest dissociation barrier (44.5 kcal/mol). Dissociation channels that feature CO and CO_2 elimination on the ground state (analogous to that in phenol and benzoic acid) have relatively large energy barriers and therefore cannot compete with H_2O elimination.

B. Conformationally controlled photodissociation dynamics

Energy for photoexcitation is usually much larger than the barrier between conformers. Fast equilibrium between various conformers occurs. Therefore, similar photochemical properties for different conformers are expected. Only few examples of conformation-selective photodissociation have been observed. One is the photodissociation of formic acid in solid Ar.[24] *Cis* formic acid was shown to preferentially dissociate upon UV photolysis into H_2 and CO_2, whereas the *trans* isomer dissociated into H_2O and CO. The dissociation mechanism remains unclear. Dissociation on the ground state due to the "conformation memory" has been proposed. However, theoretical calculations suggest that interconversion between *cis* and *trans* conformers on the ground state is faster than the dissociation processes.[39] Therefore, dissociation on the ground state cannot produce the different products for *cis* and *trans* conformers, respectively. The confinement by the

matrix material, or the dynamics on the S_1 state was proposed to explain the results.

Park and co-workers reported distinct kinetic energy release in dissociation of specific iodopropane ion conformers prepared by mass analyzed threshold ionization.[25] Thermodynamic arguments and *ab initio* calculations indicate that this difference in kinetic energy release results from different reaction channels, with gauche-1-iodopropane ions forming 2-propyl ions and anti-1-iodopropane ions forming protonated cyclopropane ions. They ascribed this result to either the H-atom migration or methyl group movement during the C-I bond cleavage on the repulsive excited states.

In another study, ion imaging experiment reveals distinct photodissociation dynamics for propanal cations initially prepared in either the *cis* or gauche conformation.[26] Gauche propanal cations dissociate into both hydroxyallyl cations and propanoyl cations, whereas *cis* propanal cations strongly favor formation of hydroxyallyl cations. This was attributed to the distinct ultrafast dynamics in the repulsive-like excited state along the H or CH_3 migration, which deposits each conformer in isolated regions of the ground-state potential energy surface. From these distinct regions, conformer interconversion does not effectively compete with dissociation.

Excited state enol-keto isomerization in 2HBA has been studied in a supersonic jet expansion.[40] Two carboxylic group rotamers of 2HBA with significantly different photophysical properties are found. 2HBA-1, the major form of 2HBA in the expansion, can undergo excited state tautomerization reaction. A nonradiative decay process with an activation energy of ~1100/cm is deduced from an abrupt decrease in fluorescence lifetimes above this energy. The other rotamer, 2HBA-2 cannot undergo excited state tautomerization.

Theoretical calculations have been performed on the excited-state intramolecular proton transfer in 2HBA-1.[41] In one study, hydrogen transfer (PT) curves have been computed for two excited states. An essentially barrierless and very shallow energy profile has been found for the $\pi\pi^*$ state. For the $n\pi^*$ state the keto minimum is more pronounced than for the $\pi\pi^*$ state and, depending on the case, energy barriers ranging from values <0.1–0.5 eV were found. In the other study of 2HBA,[42] hydrogen transfer along the intramolecular hydrogen bond as well as torsion and pyramidization of the carboxy group have been identified as the most relevant photochemical reaction coordinates. The keto-type planar S_1 state reached by barrierless intramolecular hydrogen transfer represents a local minimum of the S_1 energy surface, which is separated by a very low barrier from a reaction path leading to a low-lying S_1–S_0 conical intersection via torsion and pyramidization of the carboxy group. Similar excited state hydrogen transfer along the intramolecular hydrogen bond has been found in many other molecular systems.[43,44]

Our investigation shows that the repulsive excited state potential energy surface also plays an important role in the photodissociation of HBA. However, the mechanism for conformation dependence of HBA photodissociation is not exactly the same as those two examples described above. Photoexcitation of HBA does not directly reach the repulsive potential energy surface. Population transfer from a stable, bright state to a dark, repulsive state is necessary for dissociation on repulsive potential energy surface. There are several processes compete with each other. Excited state hydrogen transfer along the intramolecular hydrogen bond followed by internal conversion to the ground state for 2HBA-1 is much faster than the interconversion from conformer 2HBA-1 to conformer 2HBA-3. It is also faster than the population transfer from the bound state to the repulsive state. On the other hand, population transfer to the repulsive state is much faster than internal conversion for conformers without intramolecular hydrogen bonding, like 3HBA and 4HBA.

C. Implications of intramolecular hydrogen bonding effects on photostability of amino acid chromophores

The PES of phenol and phenol with intermolecular hydrogen bonding, like phenol-$(NH_3)_n$ and phenol-$(H_2O)_n$ clusters, have been reported.[7] The second excited state becomes a bound state for these clusters. It crosses the first excited state, but does not cross the ground state. The PES of the second-excited state shows that the conformation with the hydrogen-bonded H atom on the NH_3 (or H_2O) side, like C_6H_5O–H–NH_3 (or C_6H_5O–H–OH_2), is more stable than the conformation with the H atom on the phenol side, like C_6H_5O–H–NH_3 (C_6H_5O–H–OH_2). The population on the first excited state from photoexcitation can be transferred to the second excited state through the crossing between these two states, followed by hydrogen atom transfer on the second excited state. However, as the distance between phenol and NH_3 increases, the second excited state becomes repulsive, and these clusters dissociate into phenoxy radical and $(NH_3)_nH$ or $(H_2O)_nH$.

Unlike these clusters with intermolecular hydrogen bonding, the distance between hydrogen bond donor and acceptor for molecules like 2-HBA-1 with intramolecular hydrogen bonding cannot change significantly. Dissociation on the excited state would not happen for these molecules. Internal conversion followed by dissociation on the ground state becomes the major channels for the conformers of 2-HBA with intramolecular hydrogen bonding. Under collisionless conditions (as in a molecular beam and low pressure gas phase) HBA molecules absorbing UV photons will eventually dissociate into fragments, either from an excited state (for conformers of HBA without intramolecular hydrogen bonding) or the ground state (for conformers of HBA with intramolecular hydrogen bonding). Dissociation on the ground state is relatively slow and can easily be quenched in collision conditions (as in the condensed phase) by rapid intermolecular energy transfer. On the other hand, dissociation from a repulsive excited state is swift and is not readily quenched by collisions. Consequently, conformers of HBA with intramolecular hydrogen bonding would not dissociate into fragments as readily as those conformers without intramolecular hydrogen bonding in collision conditions.

These photochemistry properties are not likely limited to HBA. In general, the formation of zwitterionic species for molecules initially having intramolecular hydrogen-bonding easily gives rise to the noncrossing between the repulsive excited state and the ground state, resulting in the shutdown of dissociation from the repulsive excited state. This noncross-

ing provides an alternative mechanism for the photostability of amino acid chromophores upon irradiation of UV photons.

ACKNOWLEDGMENT

The work was supported by the National Science Council Taiwan, under contract NSC 97-2628-M-001-011-MY3 and NSC-97-2113-M-194-004. We thank the National Center for High-Performance Computing (NCHC) for providing part of computing resources.

[1]M. B. Robin, *Higher Excited States of Polyatomic Molecules* (Academic, New York, 1972).
[2]C. E. Crespo-Hernandez, B. Cohen, P. M. Hare, and B. Kohler, Chem. Rev. (Washington, DC) **104**, 1977 (2004).
[3]R. Callis, Annu. Rev. Phys. Chem. **34**, 329 (1983).
[4]D. Creed, Photochem. Photobiol. **39**, 537 (1984).
[5]A. Reuther, H. Iglev, R. Laenen, and A. Laubereau, Chem. Phys. Lett. **325**, 360 (2000).
[6]A. L. Sobolewski and W. Domcke, Chem. Phys. **259**, 181 (2000).
[7]A. L. Sobolewski and W. Domcke, J. Phys. Chem. A **105**, 9275 (2001).
[8]A. L. Sobolewski and W. Domcke, C. Dedonder-Lardeux, and C. Jouvet, Phys. Chem. Chem. Phys. **4**, 1093 (2002).
[9]B. O. Roos, P. A. Malmqvist, V. Molina, L. Serrano-Andres, and M. Merchan, J. Chem. Phys. **116**, 7526 (2002).
[10]Z. G. Lan, W. Domcke, V. Vallet, A. L. Sobolewski, and S. Mahapatra, J. Chem. Phys. **122**, 224315 (2005).
[11]C. M. Tseng, Y. T. Lee, and C. K. Ni, J. Chem. Phys. **121**, 2459 (2004); C. M. Tseng, Y. T. Lee, M. F. Lin, C. K. Ni, S. Y. Liu, Y. P. Lee, Z. F. Xu, and M. C. Lin, J. Phys. Chem. A. **111**, 9463 (2007).
[12]M. F. Lin, C. M. Tseng, Y. T. Lee, and C. K. Ni, J. Chem. Phys. **123**, 124303 (2005).
[13]M. G. D. Nix, A. L. Devine, B. Cronin, R. N. Dixon, and M. N. R. Ashfold, J. Chem. Phys. **125**, 133318 (2006).
[14]M. N. R. Ashfold, B. Cronin, A. L. Devine, R. N. Dixon, and M. G. D. Nix, Science **312**, 1637 (2006).
[15]M. J. Tubergen, J. R. Cable, and D. H. Levy, J. Chem. Phys. **92**, 51 (1990).
[16]L. C. Snoek, R. T. Kroemer, M. R. Hockridge, and J. P. Simons, Phys. Chem. Chem. Phys. **3**, 1819 (2001).
[17]G. Rouille, M. Arnold, A. Staicu, T. Henning, and F. Huisken, J. Phys. Chem. A **113**, 8187 (2009).
[18]A. Lindinger, P. J. Toennies, and A. F. Vilesov, J. Chem. Phys. **110**, 1429 (1999).
[19]Y. Inokuchi, Y. Kobayashi, T. Ito, and T. Ebata, J. Phys. Chem. A **111**, 3209 (2007).
[20]L. C. Snoek, E. G. Robertson, R. T. Kroemer, and J. P. Simons, Chem. Phys. Lett. **321**, 49 (2000).
[21]B. C. Dian, A. Longarte, S. Mercier, D. A. Evans, D. J. Wales, and T. S. Zwier, J. Chem. Phys. **117**, 10688 (2002).
[22]B. C. Dian, A. Longarte, and T. S. Zwier, J. Chem. Phys. **118**, 2696 (2003).
[23]D. Shemesh, A. L. Sobolewskib, and W. Domcke, Phys. Chem. Chem. Phys. **12**, 4899 (2010).
[24]L. Khriachtchev, E. Macoas, M. Pettersson, and M. Rasanen, J. Am. Chem. Soc. **124**, 10994 (2002).
[25]S. T. Park, S. K. Kim, and M. S. Kim, Nature **415**, 306 (2002).
[26]M. H. Kim, L. Shen, H. Tao, T. J. Martinez, and A. G. Suits, Science **315**, 1561 (2007).
[27]S. T. Tsai, C. K. Lin, Y. T. Lee, and C. K. Ni, J. Chem. Phys. **113**, 67 (2000).
[28]S. T. Tsai, C. K. Lin, Y. T. Lee, and C. K. Ni, Rev. Sci. Instrum. **72**, 1963 (2001).
[29]C. K. Ni and Y. T. Lee, Int. Rev. Phys. Chem. **23**, 187 (2004).
[30]A. D. Becke, J. Chem. Phys. **98**, 5648 (1993).
[31]C. Lee, W. Yang, and R. G. Parr, Phys. Rev. B **37**, 785 (1988).
[32]A. G. Baboul, L. A. Curtiss, P. C. Redfern, and K. Raghavachari, J. Chem. Phys. **110**, 7650 (1999).
[33]L. A. Curtiss, K. Raghavachari, P. C. Redfern, A. G. Baboul, and J. A. Pople, Chem. Phys. Lett. **314**, 101 (1999).
[34]M. J. Frisch, G. W. Trucks, H. Schlegel *et al.*, Gaussian 03, Revision C.02, Gaussian, Inc., Wallingford, CT, 2004.
[35]MOLPRO, version 2009.1, designed by H.-J. Werner and P. J. Knowles (2009).
[36]R. E. Stratmann, G. E. Scuseria, and M. J. Frisch, J. Chem. Phys. **109**, 8218 (1998).
[37]See supplementary material at http://dx.doi.org/10.1063/1.3526059 for (a) mass spectra of 2-, 3-, 4-HBA in a molecular beam. (b) Mass spectra of photofragments from photodissociation of 2-, 3-, 4-HBA in a molecular beam at 193 nm. (c) Structures, energies of various conformers and barriers of 3-, 4-HBA. (d) Potential energy surfaces of 2-HBA-1 along O-H bond distance and the angle between O-H axis and the plane of aromatic ring. (e) Energies of the ground state and singlet excited states along the O-H bond distance in carboxyl group for 2HBA-1. (f) Potential energies of intermediates, transition states, and products for various dissociation channels of 3-, 4-HBA on the electronic ground state.
[38]Y. A. Dyakov, A. Bagchi, Y. T. Lee, and C. K. Ni, J. Chem. Phys. **132**, 014305 (2010).
[39]E. Martinez-Nunez, S. A. Vazquez, I. Borges, Jr., A. B. Rocha, C. M. Estevez, J. F. Castillo, and F. J. Aoiz, J. Chem. Phys. **109**, 2836 (2005).
[40]P. B. Bisht, H. Petek, K. Yoshihara, and U. Nagashima, J. Chem. Phys. **103**, 5290 (1995).
[41]A. J. A. Aquino, H. Lischka, and C. Hattig, J. Phys. Chem. A **109**, 3201 (2005).
[42]A. L. Sobolewski and W. Domcke, Phys. Chem. Chem. Phys. **8**, 3410 (2006).
[43]A. L. Sobolewski and W. Domcke, J. Phys. Chem. A **111**, 11725 (2007).
[44]J. M. Ortiz-Sánchez, R. Gelabert, M. Moreno, and J. M. Lluch, J. Chem. Phys. **127**, 084318 (2007).